HHS Public Access

Author manuscript

Biomaterials. Author manuscript; available in PMC 2017 September 01.

Published in final edited form as:

Biomaterials. 2016 September ; 102: 175–186. doi:10.1016/j.biomaterials.2016.06.031.

Nanoparticle tumor localization, disruption of autophagosomal trafficking, and prolonged drug delivery improve survival in peritoneal mesothelioma

Rong Liu[1,‡], **Aaron H. Colby**[1,2,‡], **Denis Gilmore**[1], **Morgan Schulz**[1], **Jialiu Zeng**[2], **Robert F. Padera**[3], **Orian Shirihai**[4,5], **Mark W. Grinstaff**[2,*], and **Yolonda L. Colson**[1,*]

[1]Department of Surgery, Brigham and Women's Hospital, Harvard Medical School, Boston, MA, USA

[2]Departments of Biomedical Engineering and Chemistry, Boston University, Boston, MA, USA

[3]Department of Pathology, Brigham and Women's Hospital, Harvard Medical School, Boston, MA, USA

[4]Department of Medicine, Obesity and Nutrition Section, Evans Biomedical Research Center, Boston University School of Medicine, Boston, MA, USA

[5]Department of Clinical Biochemistry, School of Medicine, Ben Gurion University, Beer-Sheva, Israel

Abstract

The treatment outcomes for malignant peritoneal mesothelioma are poor and associated with high co-morbidities due to suboptimal drug delivery. Thus, there is an unmet need for new approaches that concentrate drug at the tumor for a prolonged period of time yielding enhanced antitumor efficacy and improved metrics of treatment success. A paclitaxel-loaded pH-responsive expansile nanoparticle (PTX-eNP) system is described that addresses two unique challenges to improve the outcomes for peritoneal mesothelioma. First, following intraperitoneal administration, eNPs rapidly and specifically localize to tumors. The rate of eNP uptake by tumors is an order of magnitude faster than the rate of uptake in non-malignant cells; and, subsequent accumulation in autophagosomes and disruption of autophagosomal trafficking leads to prolonged intracellular retention of eNPs. The net effect of these combined mechanisms manifests as rapid localization to intraperitoneal tumors within 4 hrs of injection and persistent intratumoral retention for > 14 days.

[*]Corresponding authors: Yolonda L. Colson, M.D., Ph.D., ycolson@partners.org, Department of Surgery, Brigham and Women's Hospital, Harvard Medical School. 75 Francis St, Boston, MA 02115, Phone: 617-732-6648; Mark W. Grinstaff, Ph.D., mgrin@bu.edu, Departments of Biomedical Engineering and Chemistry, Boston University. 590 Commonwealth Avenue, Room #518, Boston, MA 02215, Phone: 617-358-3429.

[‡]contributed equally to the work

Disclosure of Conflicts of Interest: No potential conflicts of interest were disclosed.

Author contributions: RL, AHC, MWG and YLC designed the research; RL, AHC, MS, DG and JZ conducted the research; RL, AHC, JZ, RFP, OS, MWG and YLC analyzed the data; RL, AHC, MWG and YLC wrote the Manuscript.

Second, the high tumor-specificity of PTX-eNPs leads to delivery of greater than 100 times higher concentrations of drug in tumors compared to PTX alone and this is maintained for at least seven days following administration. As a result, overall survival of animals with established mesothelioma more than doubled when animals were treated with multiple doses of PTX-eNPs compared to equivalent dosing with PTX or non-responsive PTX-loaded nanoparticles.

Keywords

mesothelioma; nanoparticle; drug delivery; paclitaxel; autophagosome; tumor localization

1. Introduction

Unlike other solid cancers where mortality commonly results from metastatic disease, patients with diffuse peritoneal malignancies often succumb to local disease progression and locoregional recurrence. The rapid local progression of mesothelioma results in a median survival of only 4-12 months following diagnosis, even with best supportive care [1-3], while systemic intravenous platinum-based chemotherapy alone offers minimal improvement [4]. Therefore, peritoneal mesothelioma, as well as other peritoneal malignancies such as ovarian, gastric, and appendiceal carcinoma, are sometimes treated with multimodality regimens consisting of cytoreductive surgery followed by intracavitary chemotherapy with the goal of ablating residual microscopic tumor [5-9]. Aggressive surgical debulking and intraoperative heated chemotherapy have been advocated for the treatment of both intraperitoneal and intrapleural malignant mesothelioma since large bulky tumors and massive pleural effusions and/or ascites severely compromise quality of life in these patients. Interestingly, due to the unique pharmacokinetics of the peritoneal-plasma barrier, clinical trials investigating intraperitoneal, rather than IV, chemotherapy demonstrate improved survival and increased intratumoral drug levels with comparatively fewer systemic side effects [10-12]. However, despite initial palliation of symptoms, the majority of patients still succumb to unrelenting locoregional tumor growth, with significant financial and emotional cost [13]. Given the high incidence of local disease failures and the rapid clearance of systemically administered paclitaxel, the treatment regimen of these patients now includes five consecutive days of intraperitoneal paclitaxel, in an attempt to keep drug levels high following surgical debulking and intra-operative chemotherapy. Cure has been reported in some patients, although the overall 5-year survival remains poor [14-18].

Given the challenge of local tumor recurrence, novel locoregional therapies are being investigated. These include mesothelin-targeted immunotherapy, which has prolonged survival in animal models of pleural mesothelioma [13], and various micro- and nanoparticle (NP) drug delivery systems designed to address many of the limitations that currently prevent optimal delivery of more traditional chemotherapeutic agents to tumors. Particle-based systems are being engineered to: increase the solubility of hydrophobic drugs; provide more consistent drug levels over prolonged periods; protect sensitive drugs from degradation or enzymatic alteration; and, in some cases, provide local or “targeted” delivery to a desired tissue [19-27]. Drug delivery systems using particles, nanorods, micelles, or hydrogels, have been developed specifically for the treatment of peritoneal carcinomatoses [28-33], with

poly(lactic acid) (PLA) and poly(lactic-*co*-glycolic acid) (PLGA) being the most widely studied formulations due to availability, biocompatibility, and use in other FDA approved devices [34-36]. Unfortunately, the rapid "burst" release of >50% of encapsulated drug within the first 10-48 hrs prevents the clinical application of these formulations in the setting of large debulking operations as post-operative healing is critical and sustained drug release is required to kill tumor cells with extended doubling times [37, 38]. To address these shortcomings, functional systems in which drug release is triggered by specific physical stimuli (e.g., pH, temperature, oxidative/reductive environments, or osmolality) are being pursued to improve the anti-tumor efficacy of NP-based therapies [39-41].

In this manuscript, we describe an efficacious, pH-responsive, expansile nanoparticle (eNP) drug-delivery system and investigate three unique aspects of this system including: the surprisingly discordant relationship between *in vitro* and *in vivo* efficacy, the mechanism of tumor-specific localization *in vivo*, and enhanced anti-tumor efficacy *in vivo*. First, we developed a "short duration-of-exposure" *in vitro* cytotoxicity assay model that more accurately mimics the rapid clearance of PTX *in vivo* and evaluated PTX-eNPs and PTX in both this and conventional models. Second, we investigated the kinetics and mechanisms of intratumoral eNP accumulation by characterizing the disparity in the rate of eNP internalization in native versus malignant peritoneal cells as well as the accumulation in autophagosomes and disruption of autophagosomal degradation/flux. Third, given that prolonged low drug concentrations may actually prove detrimental by facilitating the selection and growth of cancer stem cells [42, 43]—we explored the ramifications of sustained high PTX concentrations over multiple cell cycles using a multiple-dose *in vivo* model of human mesothelioma. We hypothesized that PTX-eNPs would prove superior to an equivalent PTX dose due to enhanced prolonged intratumoral delivery of PTX and, thus, significantly improve the survival of animals even with established human mesothelioma tumors.

2. Materials and methods

2.1. Nanoparticle Synthesis and Characterization

Expansile nanoparticles (eNPs), non-expansile nanoparticles (neNPs) and poly(lactic-*co*-glycolic) acid (MW ∼50-80k) nanoparticles (PLGA-NPs) with or without paclitaxel (PTX-eNP and PTX-PLGA-NPs) were prepared using a previously reported mini-emulsion technique with base-catalyzed polymerization of eNPs and neNPs [30, 44-46]. Briefly, nanoparticle monomer and crosslinker (or polymer in the case of PLGA) with or without paclitaxel were dissolved in 500 uL of dichloromethane. This was combined with 2 mL of 10 mM pH 7.4 phosphate buffer containing 8 mg/mL sodium dodecyl sulfate and sonicated under argon for 30 minutes using a Sonotek probe sonicator with 20% amplitude and a 1 second on 2 seconds off pulse with water bath cooling. Polymerization of eNPs and neNPs was carried out by addition of 2 uL tetramethylethylenediamine and 20 uL of 200 mM ammonium persulfate. Particles were stirred under argon for 1 hr and then under air overnight. Particles were dialyzed in 5 mM pH 7.4 phosphate buffer for 24 hrs in 10,000 MWCO snakeskin dialysis tubing and the buffer (1L volume) was exchanged once after 4 hrs. Particles' PTX encapsulation efficiency was determined by quantifying PTX

concentration by high performance liquid chromatography (HPLC) as previously reported [47]. PTX alone was formulated in a 50/50 mixture of Cremophor El/ethanol (i.e., a recapitulation of Taxol®, the clinical formulation of PTX).

Fluorescently labeled eNPs were prepared by incorporating 0.02% (w/w) PolyFluor™ 407 (9-anthracenylmethyl methacrylate; PF-eNPs) or PolyFluor™ 570 (methacryloxyethyl tricarbonyl rhodamine B; Rho-eNPs) into the polymer backbone during polymerization. Fluorophores were aliquotted from a 10 mg/mL stock in dimethylsulfoxide. Rhodamine-conjugated fluorescent PLGA was purchased from PolySciTech and mixed with PLGA in a 1:5 ratio to yield the final fluorescently labeled Rho-PLGA-NPs with equivalent fluorescent intensity of Rho-eNPs and Rho-neNPs.

Nanoparticles were characterized by dynamic light scattering by diluting 10 uL of particles in 3 mL of de-ionized water and measuring the hydrodynamic radius (by number) using a Brookhaven 90Plus particle sizer. Scanning electron microscopy was performed by drying a 10 uL droplet of the same particle dilution on a silicon wafer, sputter coating with Au/Pd, and imaging on a Zeiss Supra 40 scanning electron microscope.

2.2. Cell Lines

Human malignant pleural mesothelioma cells (MSTO-211H), firefly luciferase gene transfected MSTO-211H cells (MSTO-211H-Luc; a generous gift from J. Rheinwald at Harvard Medical School, Boston, MA), and healthy mesothelial cells (LP-3) were maintained at 37 °C in 5% CO_2 in complete culture media using RPMI 1640 or DMEM media, respectively, containing 10% (v/v) fetal bovine serum, streptomycin (100 mg/mL), and penicillin (100 units/mL).

2.3. In Vitro Cell Viability

MSTO-211H tumor cells were seeded in 96-well plates at 2,000 cells/well in media. After 24 hrs, media was replaced with media containing PTX-eNPs, unloaded-eNPs, or PTX. Treatment with equivalent PTX doses were determined based on encapsulation efficiency. Cells were incubated with treatments for 4 hrs and washed thrice with phosphate buffered saline (PBS) before addition of media without treatments. After further culturing for 3 days, cell viability was determined using the CellTiter 96® Aqueous One Solution Cell Proliferation Assay (MTS) (Promega, Madison, WI). Continuous treatment assays were performed under identical conditions except that treatments remained on the cells for three consecutive days (72 hrs) followed immediately by MTS assay. All viability assays were performed in triplicate and percent viability was calculated as absorbance relative to control wells receiving no treatments.

2.4. Quantification of eNP Uptake in Vitro by Flow Cytometry

Flow cytometry was used to quantify the cellular uptake of Rho-eNPs in MSTO-211H human mesothelioma tumor cells and healthy LP-3 mesothelial cells. Cells were seeded in 6-well plates at 200,000 cells/well in media and allowed to adhere and grow for 24 hrs. Media was replaced with 2 mL of media containing 50 μg/mL Rho-NPs (polymer concentration) and cells were incubated for 0, 2 or 8 hrs. At each time point, media was

removed, cells washed thrice with PBS, and fixed in 4% formaldehyde prior to analysis using a BD LSRFortessa flow cytometer (BD Biosciences). Data were analyzed using FlowJo Software (Version 10). Studies involving inhibitors were conducted under identical conditions with cells pre-treated for 1 hr with inhibitors at the maximum concentration that yielded at least 80% cell viability [48].

2.5. Characterization and Quantification of LC3-II and p62

LC3-II and p62 protein accumulation as a result of eNP treatment was determined via confocal microscopy and Western Blot. MSTO-211H cells were cultured with Rho-eNPs for confocal studies or unlabeled-eNPs, neNPs or PLGA-NPs for Western Blot as described above at concentrations of 50 ug/mL or 100 ug/mL. After 24 hrs of co-culture, cells were fixed, stained with nuclear stain (Hoescht), cell wall (Concanavalin A 633) and LC3A/B primary and AlexaFluor 488 secondary antibodies, and imaged using a Zeiss Axiovert inverted microscope. The concentration and duration of staining was performed using the company recommended values for each stain. For bafilomycin treatments, 200 nM bafilomycin was applied for 2 hrs before cell lysis. For Western blots, protein samples were extracted by lysing the cells with RIPA buffer (Santa Cruz), together with 2% Triton-X-100 and protease inhibitors (Santa Cruz). Bicinchoninic acid assay (Pierce Chemical, Rockford, IL) was used to determine total protein concentrations. Equal amounts of total protein were loaded into 4-12% polyacrylamide gels (Invitrogen) and transferred onto a polyvinylidene difluoride membrane (Invitrogen). The membranes were blocked with 5% nonfat dry milk for 1 hour and then incubated with LC3-II, p62 and GAPDH (Cell Signaling, Billerica, MA) primary antibodies according to the manufacturer's instructions overnight. Membranes were then incubated with anti-rabbit IgG secondary antibody (Cell Signaling, Billerica, MA) solution for 1 hour, and exposed to a chemiluminescent SuperSignal West Femto Maximum Sensitivity Substrate (Thermo Scientific) to detect the protein signals. Densitometric analysis of the Western blot signals was analyzed using ImageJ, and values obtained from GAPDH were used for adjustment of any differences in loading.

2.6. In Vivo Tumor Model

All animal studies utilized a murine model of established mesothelioma. Briefly, 6-8 week old, female, athymic, nude (NU/J) mice from Jackson Laboratory were housed under sterile conditions. Animal care and procedures were conducted with Institutional Animal Care and Use Committee approval, in strict compliance with all federal and institutional guidelines for the care and use of laboratory animals (Dana-Farber Cancer Institute, Boston, MA). Mice received an intraperitoneal (IP) injection of 5×10^6 MSTO-211H or MSTO-211H-Luc cells yielding established tumors within 7-10 days of xenografting.

2.7. In Vivo Localization of eNPs to Tumors

Seven days after xenografting, animals received an intraperitoneal injection of 250 mg/kg PF-eNPs diluted to 300 μL with saline. At 1, 4, 24, 72 hrs, or 14 days following PF-eNP injection, mice received an IP injection of 2.25 mg firefly luciferin prior to bioluminescent imaging with a Xenogen IVIS-50 bioluminescence camera using a 10 s exposure time. Animals were then sacrificed and high-resolution digital photographs were taken of the intraperitoneal space using a Canon PowerShot A640 camera under ambient and ultraviolet

(254 nm) light from a Wood's lamp. These studies were repeated with Rho-eNPs, Rho-neNPs and Rho-PLGA-NPs and localization evaluated at the 24 hr time point.

2.8. Paclitaxel Tissue Concentration

Two weeks following xenografting, animals received IP injections of PTX-eNPs, PTX alone, or PTX-PLGA-NPs (equivalent PTX dose of 10 mg/kg for all treatments). In the first study, animals were sacrificed three days following injection of the respective drug treatment and all visible tumor was harvested in a blinded fashion. In the second study, samples were collected at different time points following IP injection. Blood samples were collected from the tail vein in live animals under Isoflorane anesthesia. After euthanasia, 1 mL of cold PBS (Ca^{2+} and Mg^{2+} free) was used to lavage the peritoneal cavity and subsequently all visible tumor was harvested in a blinded fashion.

PTX tissue concentrations were measured by Apredica Inc (Watertown, MA) and Bioanalytical Systems Inc. (West Lafayette, IN) using LC-MS. Briefly, PTX was extracted from the tissue using an acetonitrile incubation for 30 min followed by centrifugation for 5 min at 14k RPM to remove precipitate. Supernatant was analyzed by LC-MS using an Agilent 6410 mass spectrometer coupled with an Agilent 1200 HPLC and a CTC PAL chilled autosampler, all controlled by MassHunter software. After separation on a C18 reverse phase HPLC column, peaks were analyzed by mass spectrometry (MS) using ESI ionization in MRM mode. The limit of detection was 13.5 ng/g tissue.

2.9. Multiple-Dose Models Treating Established Disease

One week following xenografting, tumor burden was confirmed via bioluminescent imaging prior to IP injection of various PTX formulations or controls. In the first four-dose study, animals received four weekly treatments of PTX-eNPs, PTX-PLGA-NPs, PTX or their respective controls of eNPs, PLGA-NPs, or saline. All PTX treatments were given IP at 10 mg/kg/wk (∼250 μg PTX/injection) totaling 1 mg over four weeks. Long-term survival was assessed with daily follow-up and individual sacrifice upon evidence of morbid disease progression. In the follow-up high-dose study, animals received four weekly injections of PTX-eNPs, eNPs, or PTX but with a dose of 20 mg/kg/wk totaling 2 mg over four weeks. Lastly, in the eight-dose study, animals received eight weekly injections of the original low dose (10 mg/kg/wk) PTX-eNPs, eNPs, or PTX regimens totaling 2 mg over the eight weeks. All injections were in a 300 μL volume.

2.10. Statistical analysis

Data are presented as mean ± standard deviation unless specified in the text. Overall survivals were described by the Kaplan-Meier method and compared via log-rank test. All computations were done in SAS v9.2 for Unix or Prism 5.0 software. All significance tests and quoted *P*-values are two-sided with $P < 0.05$ being significant.

3. Results

Expansile nanoparticles (eNPs), PTX-eNPs, Rho-eNPs, PF-eNPs, and non-swelling NP formulations (PLGA-NPs, PTX-PLGA-NPs, Rho-PLGA-NPs; “non-expansile

nanoparticles"[49]—neNPs and Rho-neNPs) were prepared as outlined above and analyzed for quality control measures. eNPs, neNPs and PLGA-NPs consist of two populations with the majority of particles in the 20-50 nm range and a smaller subset of 100-300 nm particles (SI Fig. 1). eNPs have previously been shown to expand at a mildly acidic pH (∼5), as found within the cellular endosome, and to release PTX in a pH and time-dependent manner with negligible release of PTX over 24 hrs at pH 7.4 and significant, triggered-release of >80% within 24 hrs at pH 5 [30, 44, 46, 47]. In contrast, PTX-neNPs and PTX-PLGA-NPs exhibit rapid burst release of PTX (>60% in the first 6-12 hrs) *regardless* of the pH of the surrounding environment or the proximity of the particle to the tumor [50]. The encapsulation efficiency of PTX in NPs loaded with 5% PTX by weight, as determined by HPLC, was in agreement with previous studies at ≥ 80% for all particle formulations. Non-encapsulated PTX was administered (*in vitro* and *in vivo*) as a solution of PTX in 50/50 Cremophor EL/ethanol (i.e., equivalent to the clinical formulation of Taxol®).

3.1. Demystifying the Paradox of PTX-eNP Cytotoxicity in Vitro

MSTO-211H human mesothelioma tumor cells were exposed *in vitro* to PTX-eNPs, unloaded-eNPs (vehicle control), or an equivalent dose of PTX alone for 4 hrs to simulate the *in vivo* scenario of fast clearance and short effective drug exposure time. Cells were then washed and cultured for three days before assessing cell viability in a standard MTS assay. In this short-duration exposure, PTX-eNPs were significantly more cytotoxic to MSTO-211H tumors cells than PTX (Fig. 1, solid curves. IC_{50} = 44.6 ng/mL vs 1,009 ng/mL, respectively; $P < 0.01$). In comparison to the standard *in vitro* cytotoxicity testing of continuous PTX exposure for 72 hrs (Fig. 1, dashed curves), short-duration treatment with only a 4 hr exposure to PTX was significantly less effective resulting in a 153-fold increase in IC_{50} (i.e., decrease in potency). In contrast, the IC_{50} of PTX-eNPs was quite similar between the 4 and 72 hrs treatments with a shift of only 1.15-fold (44.6 ng/mL to 38.7 ng/mL, respectively), suggesting that PTX-eNP reaches cytotoxic levels within tumor cells quite rapidly.

3.2. Rate of eNP Uptake in Malignant vs Healthy Cells

To quantify the rate of eNP cellular uptake, Rhodamine-labeled eNPs (Rho-eNPs) were cultured with MSTO-211H or a non-malignant human mesothelial line LP-3 for 0 (control), 2 or 8 hrs followed by washing and flow cytometric analysis. The malignant cells exhibited rapid uptake of Rho-eNPs with >98% of cells showing Rho-eNPs internalization within 2 hrs (Fig. 2). Interestingly, LP-3 uptake of Rho-eNPs was an order of magnitude slower with only 2% of cells showing internalization after 2 hrs and only 28% at 8 hrs. Pharmacologic inhibitors were used to selectively shut down endocytotic pathways (SI Fig. 2); the results showed that macropinocytosis is the primary route of eNP internalization into MSTO-211H cells.

3.3. Kinetics of Tumor-Specific eNP Accumulation

To visually track eNP distribution *in vivo*, fluorescent Polyfluor-labeled eNPs (PF-eNPs) were injected IP into mice bearing intraperitoneal xenografts established 7 days prior. At predetermined time points, tumor location was identified by bioluminescent imaging followed by euthanasia and necropsy. Gross abdominal examination under visible light

confirmed tumor location and imaging with a UV-lamp identified the location of PF-eNPs. The location of the bioluminescent signal matched areas of visible tumor, and a strong co-localization between PF-eNPs and both large and small tumor nodules was noted as early as 1-4 hrs after PF-eNP injection (Fig. 3). Interestingly, co-localization persisted for 14 days. Of note, the organs of the reticuloendothelial system (e.g., liver, spleen, kidneys) showed no overt sign of PF-eNP accumulation, as has been described with other NP formulations [51, 52]. This study was repeated with rhodamine-labeled eNPs, neNPs and PLGA-NPs (SI Fig. 3), revealing less tumoral accumulation of PLGA-NPs and a greater degree of non-specific tumor-accumulation for neNPs at the 24 hr time point.

3.4. Intracellular Accumulation of eNPs in Autophagosomes

Cellular retention and autophagosomal accumulation of eNPs was measured by tracking the LC3-II protein—a marker for autophagosomes [53]. MSTO-211H cells treated with eNPs for 24 hrs exhibited a a dose-dependent increase in LC3-II as quantified by Western Blot (SI Fig. 4A), with a dose of 100 μg/mL eNPs resulting in a greater than 4-fold increase in LC3-II compared to the untreated control. Treatment with neNPs or PLGA-NPs at equivalent concentrations demonstrated that PLGA-NPs do not increase LC3-II content while neNPs have a similar effect as eNPs (Fig. 4A).

To visually track the distribution of LC3-II, this experiment was repeated and the cells were fixed and stained for LC3-II. LC3-II was observed as bright, punctate dots co-localized with the Rho-eNP signal (SI Fig. 5B) and therefore, we confirmed that this co-localization was not due to non-specific binding between the secondary LC3-II antibody and Rho-eNPs. The distribution of LC3-II was similar to that of the positive autophagosome control—chloroquine (SI Fig. 5A), which prevents lysosomal and autophagosomal acidification thereby inhibiting autophagic flux and leading to accumulation of autophagosomes). The negative control—media alone (SI Fig. 5C)—exhibited less intense and non-specific background signal.

To investigate whether particle treatments inhibit autophagic degradation and flux, we assessed expression of p62, a protein normally degraded during autophagy when autophagosomes merge with acidic lysosomes. No differences in protein levels were observed between any particle treatment and control (SI Fig. 4B). As an alternative strategy for investigating autophagic flux, we repeated the LC3-II quantification study but co-treated the cells with the V-ATPase inhibitor bafilomycin, which inhibits lysosome acidification and thereby prevents autophagic degradation. The results are shown in SI Fig. 4C—these studies were run on the same gel as the data in Fig. 4A and the data in Fig. 4A are presented again in SI Fig. 4C for ease of comparison. Comparison of the LC3-II values between cells treated with (+) bafilomycin and cells without (-) bafilomycin reveals a significant effect in PLGA-NP-treated and neNP-treated cells. Specifically, the ratio of LC3-II in control vs. PLGA-NP-treated cells in the (-) bafilomycin group was 1:1.5 and this increased to 1:2.4 in the (+) bafilomycin group. The same trend was observed for neNPs with the ratio of LC3-II in control vs. neNP-treated cells increasing from 1:5.1 in the (-) bafilomycin group to 1:8.9 in the (+) bafilomycin group. In contrast, bafilomycin treatment did not *further* increase the

control to eNP-treatment ratio (i.e.: control vs. eNP-treated cells (-) bafilomycin = 1:6.9 while control vs. eNP-treated cells (+) bafilomycin = 1:2.2).

3.5. Quantification of Intratumoral Paclitaxel Concentrations In Vivo

In order to assess the tumor-specific accumulation and retention of PTX administered via eNPs compared to non-responsive NP or drug alone treatments, a single IP injection of PTX-eNPs, PTX-PLGA-NPs or PTX alone (10 mg/kg PTX for all treatment groups) was given to animals bearing intraperitoneal tumors previously established 2 weeks prior to treatment. Tumors were harvested three days after treatment in a blinded fashion and weighed, with PTX quantified by liquid chromatography-mass spectrometry (LC-MS). As expected, the average tumor weights for all three groups were not statistically different given the short duration of PTX exposure (518 ± 261 mg, 588 ± 165 mg, and 488 ± 163 mg for PTX-eNP, PTX-PLGA-NP, and PTX, respectively, $P > 0.05$). However, the tumor concentration of PTX was significantly higher in PTX-eNP treated mice than in either PTX-PLGA-NP or PTX treated mice (116.0 ± 66.9 μg/g vs. 25.4 ± 28.2 μg/g and 0.37 ± 0.27 μg/g, both $P < 0.05$; Fig. 5A). There was no statistical difference in PTX concentration between the PTX-PLGA-NP and PTX treated tumors. The % of the total injected dose of PTX remaining in the tumor tissue three days after treatment followed a similar trend with 20 ± 6% for PTX-eNPs vs. 6 ± 7% for PTX-PLGA-eNPs and 0.1 ± 0.1% for PTX.

In a second study, PTX concentration within the tumor, peritoneal fluid, and plasma was determined over a 7-day time-course for animals receiving PTX-eNPs or PTX (10 mg/kg PTX for both treatment groups). PTX concentrations within the tumor were significantly higher (4- to over 100-fold) in PTX-eNP treated animals compared to standard PTX treated animals at all time points from 1 hr to 7 days ($P < 0.001$, Fig. 5B) consistent with relatively rapid biologic clearance of PTX alone and significant intratumoral retention of PTX-eNPs. PTX concentrations in the intraperitoneal lavage were also an order of magnitude higher in PTX-eNP vs PTX treated mice 1, 3, and 7 days after treatment; however, there were no significant differences at 1 hr or 4 hrs after injection prior to clearance of PTX alone (Fig. 5C). Despite lower tumor PTX concentrations in mice treated with PTX alone, the plasma concentrations of PTX were significantly higher compared to PTX-eNP treatment at 1 hr and 4 hrs reflecting both its immediate and short-lived (i.e., bolus) bioavailability (Fig. 5D).

3.6. Impact of Multi-dose PTX-eNP on Survival in Setting of Established Mesothelioma In Vivo

Mice with established intraperitoneal mesothelioma xenografts were treated with four weekly doses of PTX (10 mg/kg/dose) formulated as: PTX-eNPs (experimental), PTX-PLGA-NPs (generic NP control), PTX (clinical formulation control) as well as the respective unloaded particle or vehicle controls (i.e., eNPs, PLGA-NPs), or saline (tumor growth control). All PTX treatments, regardless of formulation, improved survival compared to the saline control group (median survival 38 days; $P < 0.05$; Fig. 6A). PTX-eNP treatments resulted in the longest overall survival with a median survival of 74 days compared to either PTX-PLGA-NPs or PTX (43 days and 46 days, respectively, $P < 0.005$). PTX-PLGA-NP treatments showed no significant difference in survival compared to the same dose of PTX ($P = 0.1459$), which is consistent with the “burst” release kinetics of these

particles. The unloaded-eNPs and unloaded-PLGA-NP groups had a median survival of only 37 days and 30 days, similar to the saline control group.

To understand the impact of PTX dose, this study was repeated with PTX treatments of 20 mg/kg given on the same weekly four-dose schedule as the 10 mg/kg dose above. Since treatment with PTX-PLGA-NPs showed no improvement compared to PTX in the previous study, it was not included as a treatment group in this experiment. Despite receiving twice the total dose of PTX (20 mg/kg × 4 wks), median survival in both the PTX-eNP and PTX treated animals was slightly shorter than the previous experiment at 64 days and 36 days, respectively (Fig. 6B). This suggested that treatment failure did not result from a deficit in the local concentrations of PTX, but ultimately from failure to maintain local concentrations over a long enough period of time.

Therefore, for the third experiment, mice with established intraperitoneal mesothelioma were treated with the standard PTX dose of 10 mg/kg given on a weekly-dosing schedule but for twice as long—a total of *eight* weeks. This resulted in the same weekly dose (10 mg/kg) as the initial experiment but the same total dose (80 mg/kg) as the second experiment. Doubling the number of treatments resulted in a significantly increased median overall survival of 103 days for the PTX-eNP group vs essentially unchanged survival in the PTX group at 49 days ($P < 0.01$) (Fig. 6C). To assess biocompatibility and preliminary *in vivo* toxicity of the PTX-eNPs, abdominal tissues were harvested and prepared for histological examination. The eNPs were concentrated within tumor tissues located throughout the peritoneum. The eNPs were also seen within macrophages, and noted on or around the outside of the liver capsule, spleen, and kidney, but eNPs were not present within the parenchyma of these organs. Pathological evidence of tissue damage was sought but not found in the liver, spleen or kidneys from mice that received eight weekly-doses of PTX-eNPs (SI Fig. 6).

4. Discussion

Despite the advantages of direct tumor exposure, higher prolonged intratumoral drug concentrations, and reduced systemic side effects, intraperitoneal administration of standard chemotherapeutics has resulted in only limited improvements to survival, presumably due to the fact that the overall pharmacokinetic profile of IP drug delivery remains relatively poor [6, 7, 54]. Specifically, >95% of PTX is cleared from the peritoneal cavity within 24 hrs [55]. Such a short tumor-exposure time is particularly challenging for mitotic inhibitors, such as PTX, because they must be present in cytotoxic concentrations over multiple cell cycles (i.e., days) to achieve optimal efficacy. Additional factors limiting the effectiveness of PTX include the toxicity of the Cremophor EL excipient used to solubilize PTX and its small volume of biodistribution, which indicates that Cremophor EL is not readily taken up into tissues [55]. Hence, intracellular tissue concentrations of PTX may be limited by the very excipient used to solubilize it for administration.

Several studies have examined new carrier solutions as methods for increasing intraperitoneal dwell times of PTX. Mohamed et al. compared IP administration of PTX in a 1.5% dextrose peritoneal dialysis solution and in a high MW 6% hydroxyethyl hetastarch

solution [54]. While the hetastarch formulation maintained higher intraperitoneal PTX concentrations 12 hrs after injection, no significant difference was measured at the 24 hr time point. Tsai et al. compared intraperitoneal dwell times of PTX administered in one of three formulations: Cremophor EL, gelatin nanoparticles, or PLGA-microparticles [55]. The gelatin and Cremophor EL formulations resulted in rapid clearance of PTX from the peritoneal space (<1% of the injected dose remaining 24 hrs post injection) while PLGA-microparticles prolonged the intraperitoneal PTX dwell time. Nevertheless, even the PLGA-microparticle formulation failed to achieve significant long-term advantages with <2.5% of the injected dose remaining after 72 hrs.

To overcome the challenges of short intraperitoneal dwell times and low intratumoral accumulation we are investigating a unique NP delivery system. Expansile nanoparticles (eNPs) are synthesized from a hydrophobic pH-responsive polymer that enables encapsulation of hydrophobic payloads [30, 45, 46]. Upon exposure to the mildly acidic tumor microenvironment (pH ∼6.5) or the more acidic endosomal / lysosomal compartments within tumor cells (pH ∼5), eNPs undergo a compositional change that results in particle swelling and drug release; swollen eNPs are relatively hydrophobic and act as intracellular drug “depots” which leads to sustained delivery of PTX over even longer periods of time [44-47].

In the current manuscript, we first addressed the paradoxical results of our previous studies that demonstrated PTX-eNPs were *less* effective than PTX in the standard *in vitro* assays and yet more effective *in vivo* against human mesothelioma. It is well-established that traditional *in vitro* assays often fail to accurately model complex *in vivo* factors such as drug degradation, clearance, and biodistribution. Furthermore, traditional *in vitro* assays evaluate cell viability after days of drug exposure therein masking time-dependent effects, such as rapid clearance of cell-cycle specific drugs (e.g., PTX). In a series of studies examining the immediate and delayed cytotoxic effects of PTX, Au et al. demonstrated the importance of PTX exposure duration to its effectiveness *in vitro* [56]. Not surprisingly, exposure of several different cancer cell lines to PTX for only a short 3 hr duration was significantly less efficacious than exposure for the entire 4 day assay, resulting in a 10- to 40-fold increase in the IC_{50} with shorter exposure times [56].

To explore the paradox of why PTX-eNPs were *less* effective than PTX *in vitro* and yet *more* effective *in vivo*, we designed a similar *in vitro* assay to account for the short duration of tumor exposure of PTX that occurs *in vivo*. Cells were treated for 4 hrs with either PTX-eNPs, PTX, or unloaded-eNPs, before being washed and cultured for a total of 72 hrs vs. being treated continuously for 72 hrs (control) before being assessed for viability. As expected, three days of continuous treatment resulted in the greatest potency and the lowest IC_{50} for PTX (6.6 ng/mL). In comparison, short-duration PTX treatment was significantly less effective with a 153-fold increase in IC_{50} to 1,009 ng/mL, akin to the poor clinical efficacy seen with PTX therapy. Interestingly, PTX-eNP tumor cytotoxicity was equivalent for either a 4 hr or 72 hr exposure, with a shift in IC_{50} of only 1.15-fold (44.6 ng/mL to 38.7 ng/mL, respectively, in Fig. 1). Of significant interest was the fact that PTX-eNPs performed significantly better (23-fold lower IC_{50}) than PTX in the short-duration assays. These *in vitro* data following short-term PTX exposure concur with our current *in vivo* data described

below, in which PTX alone is shown to be cleared rapidly *in vivo*. Furthermore, the implications from this result are two-fold: 1) short drug exposure time is one of the reasons that PTX-eNPs are more effective than PTX *in vivo*; and, 2) enough PTX enters cells within 4 hrs via PTX-eNPs to achieve the equivalent cytotoxicity of a 3 day PTX-eNP exposure.

We hypothesized that the similar *in vitro* efficacy of PTX-eNPs after 4 hrs or 72 hrs was indicative of rapid cellular internalization of eNPs, which enabled the maximum therapeutic effect to manifest despite a shorter drug-exposure time. Flow cytometric analysis of the rate of eNP uptake in malignant MSTO-211H cells revealed that >98% of tumor cells internalized eNPs after only 2 hrs of co-incubation, thus confirming that rapid uptake is one of the factors contributing to the superior PTX-eNP anti-tumor efficacy noted in short-duration studies (Fig. 2A). In contrast, eNP uptake in a non-malignant human mesothelial cell line (LP-3) was an order of magnitude slower with only 2% of cells showing uptake at 2 hrs (Fig. 2B). This disparity in rates of particle internalization is consistent with the well-documented dysfunction of endosomal processes in malignant cells that leads to increased rates of endocytosis [57]. Pharmacologic inhibitors were used to identify the endocytotic pathway of eNP uptake which was demonstrated to be the non-specific, receptor-independent pathway known as macropinocytosis is the primary route (SI Fig. 2). These results are in agreement with a previous study evaluating eNP uptake in malignant MSTO-211H spheroids [58].

The differential rates of eNP uptake in malignant and healthy cells also have implications for *in vivo* tumor localization. Based upon the *in vitro* results presented above, we suspected that eNPs would localize specifically to tumors *in vivo*—an observation that was previously noted, but unexplained [30]. The localization studies of fluorescently labeled PF-eNPs into mice bearing established intraperitoneal mesothelioma clearly demonstrated that eNPs rapidly localize to tumors within 1-4 hrs of eNP injection and persist for at least two weeks (Fig. 3). Importantly, no overt particle accumulation was observed in the reticuloendothelial system (e.g., liver, spleen, kidneys). Although other polymer-based nanoparticle delivery systems have shown a degree of tumor-specificity when administered IP, differences in polymer type (eNP v. PLGA), particle size (20-200 nm v. 4-30 μm), biologic trigger of structural changes with eNP, surface charge (-46 mV v. unreported, but likely ~0 mV due to polyvinyl alcohol surfactant), and pathophysiology (mesothelioma v. ovarian and pancreatic cancer) make comparisons to the current study challenging [30, 59]. We repeated these studies using rhodamine-labeled eNP, neNP and PLGA-NP formulations with similar sizes (primarily 20-50 nm; SI Fig. 1) in order to provide a more robust basis for comparison. The PLGA-NPs serve as a “generic” non-responsive control while neNPs, which have a similar polymer structure, serve as a non-swelling control [49]. The results, which reveal less tumoral accumulation of PLGA-NPs or neNPs, suggest that while tumor-specificity is not exclusively unique to eNPs, eNPs do possess an advantage over other formulations (SI Fig. 3). However, due to the qualitative nature of these results, these results must be interpreted with caution. Future biodistribution studies with radiolabeled particles will address this question in more depth. Nevertheless, the current data provide compelling evidence for the tumor-specific localization of eNPs without the need for targeting agents or moieties, and highlights the rapid kinetics (1-4 hrs) and prolonged retention (14 days) of these unique

expansile nanoparticles within tumors. To our knowledge, this is the first study to report such prolonged retention of nanoparticles in mesothelioma tumors.

Given that lysosomes fuse with late endosomes and autophagosomes to degrade their contents, we hypothesized that the accumulation of eNPs within tumors may be indicative of eNP interference with intracellular trafficking (e.g., autophagy). Such a blockade would lead disruption of lysosome-mediated turnover and endosomal/autophagic flux and the inability to remove eNPs following particle uptake as illustrated in Figure 4B. One marker for autophagy and endosomal turnover is the LC3-II (microtubule associated protein 1A/1B light chain), which is formed following phosphatidylethanolamine conjugation to cytosolic LC3-I and is subsequently sequestered in the membranes of autophagosomes. Thus, LC3-II distribution and accumulation serves as a surrogate marker for autophagosome distribution and accumulation. To test our hypothesis, we examined the cellular accumulation and distribution of LC3-II in MSTO-211H cells following treatment with eNPs, neNPs and PLGA-NPs. Treatment with eNPs lead to a >4-fold increase in LC3-II expression by Western Blot (Fig. 4A); confocal microscopy revealed strong co-localization between fluorescent Rho-eNPs and LC3-II (SI Fig. 5). PLGA-NPs did not result in autophagosomal accumulation while the effect of neNPs was similar to that of eNPs. This suggests that the material type, rather than swelling functionality, is the primary factor modulating this particle-cell interaction. We hypothesize that the biodegradability of the polymer backbone (the PLGA backbone is composed of ester linkages while eNP and neNP backbones are non-hydrolysable hydrocarbon chains) may be a primary determining factor and this will be investigated in future studies.

Having determined that treatment with eNPs induces autophagosomal accumulation, we next sought to understand if this also leads to inhibition of autophagic degradation. We therefore quantified p62 levels as an indicator of autophagic degradation/flux. However, none of the particle treatments altered p62 expression compared to the controls (SI Fig. 4B). Nevertheless, because p62 expression can be transcriptionally regulated during autophagy this may confound the interpretation of p62 levels as an indicator of autophagic flux [60]. We therefore employed a second, standard strategy [61], co-treating the cells with particles and bafilomycin—bafilomycin is a V-ATPase inhibitor and thereby prevents acidification of lysosomes and, subsequently, the merging of lysosomes with autophagosomes resulting in the accumulation of autophagosomes (i.e., inhibition of autophagic degradation and flux).

The results in SI Figure 4C reveal a significant effect in PLGA-NP-treated and neNP-treated cells as characterized by the increases in the ratios of LC3-II in control vs. particle treated-cells treated from (-) bafilomycin to (+) bafilomycin treatments. This trend suggests that PLGA-NPs and neNPs do not inhibit autophagic degradation because co-treatment with bafilomycin leads to a further increase in LC3-II (indicating an accumulation of autophagosomes mainly due to the latter inhibition of autophagic degradation by bafilomycin and not by PLGA-NPs/neNPs). Furthermore, the data suggest that eNPs *do* inhibit autophagic degradation as the treatment with bafilomycin (which would normally inhibit autophagic degradation causing an increase in LC3-II levels) did *not further* increase LC3-II levels due to the prior and more significant block in autophagic degradation resulting from the eNP treatment. These results suggest that the swelling functionality of the eNPs is a

critical component in disrupting autophagic flux. Further investigation of the specific particle properties that impact autophagosomal accumulation and degradation/flux will be the subject of future work.

Nevertheless, the long-term accumulation of eNPs within tumors suggested that these particles may provide a means of delivering high concentrations of PTX specifically to tumor tissues over prolonged periods of time (e.g., at least a week) with a single dose. To quantify this functionality, we assessed intratumoral PTX concentrations at various time points following treatment with 10 mg/kg doses of PTX administered using eNPs, PLGA-NPs, or PTX alone. In the first study, PTX-eNPs afforded significantly greater (>100-fold) intratumoral drug concentrations at 3 days than PTX and a nearly 5-fold higher intratumoral drug concentration compared to PTX-PLGA-NPs. The second study assessed the kinetics of PTX concentrations in the tumor, intraperitoneal space/peritoneal lavage, and plasma and demonstrated that tumoral concentrations of PTX were 10-fold (at 4 hrs) to over a 100-fold higher (at 7 days) when delivered as PTX-eNPs compared to standard PTX (Fig. 5B). Interestingly, the initial bolus of PTX resulted in extremely high concentrations of drug in the intraperitoneal lavage at 1 hr and 4 hrs but this did not translate into higher intratumoral drug levels as compared to PTX-eNPs at these same two time points. These findings demonstrate that maintenance of high intraperitoneal drug levels is neither necessary, nor sufficient, to achieving high intratumoral drug levels (Fig. 5B,C). Also of note, the intraperitoneal lavage levels for PTX declined by 3-4 orders of magnitude by 24 hrs reflecting the rapid clearance of PTX from the peritoneal space. These studies demonstrate that rapid PTX clearance known to occur *in vivo* significantly reduces the available drug within 24 hours after PTX injection. This finding is in marked contrast to the persistence of significantly higher intratumoral PTX levels present even a week following PTX-eNP administration.

In comparison to other particle-based drug delivery systems under development for the treatment of peritoneal cancers, PTX-eNPs deliver significantly more drug to the tumor than other particle formulations. For example, PLGA-microparticles were designed to deliver PTX with a two-phase release profile to afford both high initial and prolonged cytotoxic concentrations [59]. Nevertheless, 3 days after an intraperitoneal injection of these PTX-loaded PLGA-microparticles, PTX concentrations in the tumor were only 13 μg/g—i.e., ∼10-fold lower than those achieved with PTX-eNPs in the current study. Importantly, these previously reported levels are in general agreement with those observed in the current study using PTX-PLGA-NPs (i.e., 25.4 ± 28.2 μg/g; Fig. 6A). The consistency between these results indicates that fundamental characteristics of the current eNP system (e.g., functionality of pH responsive swelling, tumor localization and subsequent specific drug release) are responsible for the improved, prolonged, tumor-specific delivery of PTX.

Given the higher and more prolonged intratumoral drug concentrations noted when PTX was delivered via PTX-eNPs compared to PTX in Cremophor EL, we hypothesized that PTX-eNPs would lead to improved efficacy and thus prolong survival in a murine model of human intraperitoneal mesothelioma. We have previously demonstrated that a single dose of PTX-eNPs was significantly more effective than PTX in preventing the establishment of peritoneal mesothelioma (i.e., tumor cells and treatment co-injected into the peritoneal

cavity) but treatment at the time of tumor injection is not clinically relevant [30]. In the current study, we developed a more relevant and biologically challenging model of established mesothelioma where tumors are allowed to grow for 7 days before treatment. Using this model, we performed three survival studies whose outcomes demonstrate the importance of both the formulation and treatment-schedule in maximizing PTX's therapeutic effect.

In the first study, we administered treatments once per week for four weeks to mimic the clinical treatment of mesothelioma, which employs multiple cycles of PTX to maximize its efficacy [62]. However, our analysis demonstrated that tumoral PTX levels decrease to negligible values in animals receiving weekly PTX alone but remains high between doses in animals treated with PTX-eNPs (Fig. 5B). This resulted in a significantly longer median overall survival following treatment with PTX-eNPs (72 days) vs. PTX and PTX-PLGA-NPs (46 and 43 days, respectively; $P < 0.05$). Even more impressive was that 33% of the PTX-eNP animals demonstrated a complete response at 90 days (Fig. 6A). The success of PTX-eNPs and failure of PTX-PLGA-NPs to improve survival compared to PTX demonstrates the importance of material composition and particle functionality in designing particle-based drug delivery systems. Specifically, PTX-eNPs release PTX only once they are localized to the tumor, thereby resulting in sustained, high, therapeutic intratumoral drug levels from one injection to the next. In contrast, the rapid, un-triggered, and non-specific release of PTX from PLGA-NPs that occurs within 12-24 hrs of administration is likely a critical factor in their inability to improve overall survival in the current study [38]. Not surprisingly, all PTX treatment groups exhibited statistically significant increases in survival compared to the saline control ($P < 0.05$) reflecting the clinically observed result that multiple cycles of intraperitoneal PTX assist in providing an overall survival benefit compared to treatment without intraperitoneal PTX [5].

In the second study, we explored whether the benefit of multi-dose PTX-eNPs for overall survival could be amplified by increasing the dose from 10 mg/kg/wk to 20 mg/kg/wk—a dose still within a clinically acceptable range. Both PTX-eNPs and PTX exhibited negligible benefit to overall survival indicating that dose was not the treatment-limiting factor in the previous 10 mg/kg/wk study (Fig. 6B). Furthermore, because increasing the dose is likely to lead to an initial increase in PTX concentrations in the tumor, the lack of improved survival suggests such initial increases have little effect on tumor growth. This indicates that once a cytotoxic dose is reached within the tumor that the limiting factor in improving outcomes becomes the duration of exposure to drug as additional tumor cells enter mitosis and become susceptible to PTX.

We therefore assessed the impact of a prolonged 8-week course of PTX-eNP therapy using the original 10 mg/kg/wk dosing strategy. The results support our hypothesis as median overall survival increased from 64 to 103 days for PTX-eNPs (acute v. prolonged dosing, respectively; Fig. 6C). Given the importance of both concentration and duration of exposure to the effectiveness of PTX [63, 64], the multiple order-of-magnitude increase in tumoral concentration maintained over a prolonged timeframe as described above is certainly one of the reasons for the significantly improved overall survival with PTX-eNPs as compared to PTX. Interestingly, all but one of the animals receiving PTX alone treatments died before

completing their 8-dose regimen, reflecting the lack of improvement in overall survival despite a more chronic treatment regimen. Thus, while increasing the duration of PTX exposure is essential, it is not sufficient to achieve increased survival unless sufficient concentration can also be maintained as occurs with PTX-eNPs.

Interestingly, despite the similar duration from end-of-treatment to median survival of 46 vs. 47 days, animals in the four-week group died primarily of bulky, established tumor while those in the eight-week group died bearing small tumors and/or large volume ascites. These differences in disease at the time of death suggest that PTX-eNPs have shifted the pathological mechanisms resulting in animal mortality away from the traditionally observed problem of locally recurrent bulky disease.

Importantly, taken on their own, the poor results from the PTX treatments serve to further the clinical impression that mesothelioma tends to be PTX “resistant”. However, the results from the PTX-eNP treatments reveal that this “resistance” is actually dependent on the kinetics of intra-tumoral drug delivery. Due to the improvement in pharmacokinetics and drug localization inherent in the design of PTX-eNPs, multiple injections of responsive, controlled-release PTX-eNPs are effective in prolonging overall survival *in vivo* by more than double (49 vs. 103 days), even in a traditionally “paclitaxel-resistant” tumor model.

5. Conclusions

PTX has shown clinical success in the management of mesothelioma in a subset of patients; however, current methods (i.e., bolus delivery) and routes of systemic IV or intraperitoneal administration are unable to take full advantage of PTX's therapeutic potential. In particular, maintenance of high tumor concentrations of PTX over a longer period of time is essential for maximizing the ability to effectively control and treat peritoneal mesothelioma. Broadly speaking, several of the unmet challenges in intraperitoneal drug delivery include the need for: 1) increased drug retention times in the intraperitoneal cavity to allow exposure of more mitotic tumor cells and greater penetration into tumors; 2) enhanced tumor uptake of drug and higher intratumoral concentrations; and, 3) drug delivery systems that enhance tumor-specific delivery and therein increase drug delivery into tumor cells. The PTX-eNP system described in this manuscript meets each of these criteria and, in so doing, is superior to PTX or PTX-PLGA-NPs in treating established intraperitoneal mesothelioma. The superiority of PTX-eNP treatment in animal survival vs. PTX alone is explained by data demonstrating the rapid, selective accumulation of PTX-eNP in intraperitoneal tumors, the retention of eNPs in tumors via disruption of the autophagic pathway, and the delivery of greater than 100 times PTX in the tumor for at least seven days following injection. These results demonstrate the unique functional design of the eNP delivery system, and a fundamentally different approach to intratumoral drug delivery that is a potentially viable adjunct to multimodality therapy in the treatment of malignant peritoneal mesothelioma.

Supplementary Material

Refer to Web version on PubMed Central for supplementary material.

Acknowledgments

This study is supported by the Center for Integration of Medicine and Innovative Technology, the Mesothelioma Applied Research Foundation, and the International Mesothelioma Program of the Brigham and Women's Hospital. The authors wish to express appreciation for the excellent care provided by the staff at the Animal Resources Facility at Dana-Farber Cancer Institute. We would like to thank J. Rheinwald at Harvard Medical School for the generous gift of the luciferase transfected MSTO-211H cell line. We also thank Kyle Trudeau for helpful suggestions to the figures.

References

1. Chahinian AP, Pajak TF, Holland JF, Norton L, Ambinder RM, Mandel EM. Diffuse malignant mesothelioma. Prospective evaluation of 69 patients. Ann Intern Med. 1982; 96:746–55. [PubMed: 7091938]
2. Law MR, Gregor A, Hodson ME, Bloom HJ, Turner-Warwick M. Malignant mesothelioma of the pleura: a study of 52 treated and 64 untreated patients. Thorax. 1984; 39:255–9. [PubMed: 6426072]
3. Martini N, McCormack PM, Bains MS, Kaiser LR, Burt ME, Hilaris BS. Pleural mesothelioma. The Annals of thoracic surgery. 1987; 43:113–20. [PubMed: 3541812]
4. Garcia-Carbonero R, Paz-Ares L. Systemic chemotherapy in the management of malignant peritoneal mesothelioma. Eur J Surg Oncol. 2006; 32:676–81. [PubMed: 16616827]
5. Yan TD, Welch L, Black D, Sugarbaker PH. A systematic review on the efficacy of cytoreductive surgery combined with perioperative intraperitoneal chemotherapy for diffuse malignancy peritoneal mesothelioma. Ann Oncol. 2007; 18:827–34. [PubMed: 17130182]
6. Kelly KJ, Nash GM. Peritoneal debulking/intraperitoneal chemotherapy-non-sarcoma. J Surg Oncol. 2014; 109:14–22. [PubMed: 24166680]
7. Yan TD, Cao CQ, Munkholm-Larsen S. A pharmacological review on intraperitoneal chemotherapy for peritoneal malignancy. World J Gastrointest Oncol. 2010; 2:109–16. [PubMed: 21160929]
8. Riss S, Mohamed F, Dayal S, Cecil T, Stift A, Bachleitner-Hofmann T, et al. Peritoneal metastases from colorectal cancer: patient selection for cytoreductive surgery and hyperthermic intraperitoneal chemotherapy. Eur J Surg Oncol. 2013; 39:931–7. [PubMed: 23810280]
9. Coccolini F, Cotte E, Glehen O, Lotti M, Poiasina E, Catena F, et al. Intraperitoneal chemotherapy in advanced gastric cancer. Meta-analysis of randomized trials. Eur J Surg Oncol. 2014; 40:12–26. [PubMed: 24290371]
10. Feldman AL, Libutti SK, Pingpank JF, Bartlett DL, Beresnev TH, Mavroukakis SM, et al. Analysis of factors associated with outcome in patients with malignant peritoneal mesothelioma undergoing surgical debulking and intraperitoneal chemotherapy. J Clin Oncol. 2003; 21:4560–7. [PubMed: 14673042]
11. Yan TD, Edwards G, Alderman R, Marquardt CE, Sugarbaker PH. Morbidity and mortality assessment of cytoreductive surgery and perioperative intraperitoneal chemotherapy for diffuse malignant peritoneal mesothelioma--a prospective study of 70 consecutive cases. Annals of surgical oncology. 2007; 14:515–25. [PubMed: 17031722]
12. Sugarbaker PH, Stuart OA, Vidal-Jove J, Pessagno AM, DeBruijn EA. Pharmacokinetics of the peritoneal-plasma barrier after systemic mitomycin C administration. Cancer Treat Res. 1996; 82:41–52. [PubMed: 8849942]
13. Adusumilli PS, Cherkassky L, Villena-Vargas J, Colovos C, Servais E, Plotkin J, et al. Regional delivery of mesothelin-targeted CAR T cell therapy generates potent and long-lasting CD4-dependent tumor immunity. Sci Transl Med. 2014; 6:261ra151.
14. Flores RM, Pass HI, Seshan VE, Dycoco J, Zakowski M, Carbone M, et al. Extrapleural pneumonectomy versus pleurectomy/decortication in the surgical management of malignant pleural mesothelioma: results in 663 patients. J Thorac Cardiovasc Surg. 2008; 135:620–6. [PubMed: 18329481]
15. Janne PA, Baldini EH. Patterns of failure following surgical resection for malignant pleural mesothelioma. Thorac Surg Clin. 2004; 14:567–73. [PubMed: 15559064]

16. Maggi G, Casadio C, Cianci R, Rena O, Ruffini E. Trimodality management of malignant pleural mesothelioma. Eur J Cardiothorac Surg. 2001; 19:346–50. [PubMed: 11251277]
17. Ruffie P, Feld R, Minkin S, Cormier Y, Boutan-Laroze A, Ginsberg R, et al. Diffuse malignant mesothelioma of the pleura in Ontario and Quebec: a retrospective study of 332 patients. J Clin Oncol. 1989; 7:1157–68. [PubMed: 2666592]
18. Rusch VW, Giroux D, Kennedy C, Ruffini E, Cangir AK, Rice D, et al. Initial analysis of the international association for the study of lung cancer mesothelioma database. J Thorac Oncol. 2012; 7:1631–9. [PubMed: 23070243]
19. Wang AZ, Langer R, Farokhzad OC. Nanoparticle delivery of cancer drugs. Annu Rev Med. 2012; 63:185–98. [PubMed: 21888516]
20. Petros RA, DeSimone JM. Strategies in the design of nanoparticles for therapeutic applications. Nat Rev Drug Discov. 2010; 9:615–27. [PubMed: 20616808]
21. Kieler-Ferguson HM, Frechet JM, Szoka FC Jr. Clinical developments of chemotherapeutic nanomedicines: polymers and liposomes for delivery of camptothecins and platinum (II) drugs. Wiley Interdiscip Rev Nanomed Nanobiotechnol. 2013; 5:130–8. [PubMed: 23335566]
22. Heidel JD, Davis ME. Clinical developments in nanotechnology for cancer therapy. Pharmaceutical research. 2011; 28:187–99. [PubMed: 20549313]
23. Tibbitt MW, Rodell CB, Burdick JA, Anseth KS. Progress in material design for biomedical applications. Proceedings of the National Academy of Sciences of the United States of America. 2015; 112:14444–51. [PubMed: 26598696]
24. Wang Y, Byrne JD, Napier ME, DeSimone JM. Engineering nanomedicines using stimuli-responsive biomaterials. Advanced drug delivery reviews. 2012; 64:1021–30. [PubMed: 22266128]
25. Torchilin VP. Multifunctional, stimuli-sensitive nanoparticulate systems for drug delivery. Nat Rev Drug Discov. 2014; 13:813–27. [PubMed: 25287120]
26. Jensen AI, Binderup T, Kumar EP, Kjaer A, Rasmussen PH, Andresen TL. Positron emission tomography based analysis of long-circulating cross-linked triblock polymeric micelles in a U87MG mouse xenograft model and comparison of DOTA and CB-TE2A as chelators of copper-64. Biomacromolecules. 2014; 15:1625–33. [PubMed: 24645913]
27. Morachis JM, Mahmoud EA, Almutairi A. Physical and chemical strategies for therapeutic delivery by using polymeric nanoparticles. Pharmacol Rev. 2012; 64:505–19. [PubMed: 22544864]
28. Bae WK, Park MS, Lee JH, Hwang JE, Shim HJ, Cho SH, et al. Docetaxel-loaded thermoresponsive conjugated linoleic acid-incorporated poloxamer hydrogel for the suppression of peritoneal metastasis of gastric cancer. Biomaterials. 2013; 34:1433–41. [PubMed: 23174142]
29. Bajaj G, Yeo Y. Drug delivery systems for intraperitoneal therapy. Pharmaceutical research. 2010; 27:735–8. [PubMed: 20198409]
30. Colson YL, Liu R, Southard EB, Schulz MD, Wade JE, Griset AP, et al. The performance of expansile nanoparticles in a murine model of peritoneal carcinomatosis. Biomaterials. 2011; 32:832–40. [PubMed: 21044799]
31. De Smet L, Ceelen W, Remon JP, Vervaet C. Optimization of drug delivery systems for intraperitoneal therapy to extend the residence time of the chemotherapeutic agent. ScientificWorldJournal. 2013; 2013:720858. [PubMed: 23589707]
32. Wolinsky JB, Colson YL, Grinstaff MW. Local drug delivery strategies for cancer treatment: gels, nanoparticles, polymeric films, rods, and wafers. J Control Release. 2012; 159:14–26. [PubMed: 22154931]
33. Zahedi P, Stewart J, De Souza R, Piquette-Miller M, Allen C. An injectable depot system for sustained intraperitoneal chemotherapy of ovarian cancer results in favorable drug distribution at the whole body, peritoneal and intratumoral levels. J Control Release. 2012; 158:379–85. [PubMed: 22154933]
34. Amoozgar Z, Wang L, Brandstoetter T, Wallis SS, Wilson EM, Goldberg MS. Dual-layer surface coating of PLGA-based nanoparticles provides slow-release drug delivery to achieve metronomic therapy in a paclitaxel-resistant murine ovarian cancer model. Biomacromolecules. 2014; 15:4187–94. [PubMed: 25251833]

35. Rosalia RA, Cruz LJ, van Duikeren S, Tromp AT, Silva AL, Jiskoot W, et al. CD40-targeted dendritic cell delivery of PLGA-nanoparticle vaccines induce potent anti-tumor responses. Biomaterials. 2015; 40:88–97. [PubMed: 25465442]
36. Zentner GM, Rathi R, Shih C, McRea JC, Seo MH, Oh H, et al. Biodegradable block copolymers for delivery of proteins and water-insoluble drugs. J Control Release. 2001; 72:203–15. [PubMed: 11389999]
37. Sahoo SK, Panyam J, Prabha S, Labhasetwar V. Residual polyvinyl alcohol associated with poly (D,L-lactide-co-glycolide) nanoparticles affects their physical properties and cellular uptake. J Control Release. 2002; 82:105–14. [PubMed: 12106981]
38. Xu P, Gullotti E, Tong L, Highley CB, Errabelli DR, Hasan T, et al. Intracellular drug delivery by poly(lactic-co-glycolic acid) nanoparticles, revisited. Molecular pharmaceutics. 2009; 6:190–201. [PubMed: 19035785]
39. Stuart MA, Huck WT, Genzer J, Muller M, Ober C, Stamm M, et al. Emerging applications of stimuli-responsive polymer materials. Nat Mater. 2010; 9:101–13. [PubMed: 20094081]
40. Mura S, Nicolas J, Couvreur P. Stimuli-responsive nanocarriers for drug delivery. Nat Mater. 2013; 12:991–1003. [PubMed: 24150417]
41. Felber AE, Dufresne MH, Leroux JC. pH-sensitive vesicles, polymeric micelles, and nanospheres prepared with polycarboxylates. Advanced drug delivery reviews. 2012; 64:979–92. [PubMed: 21996056]
42. Baguley BC, Finlay GJ. Pharmacokinetic/cytokinetic principles in the chemotherapy of solid tumours. Clinical and experimental pharmacology & physiology. 1995; 22:825–8. [PubMed: 8593737]
43. Abubaker K, Latifi A, Luwor R, Nazaretian S, Zhu H, Quinn MA, et al. Short-term single treatment of chemotherapy results in the enrichment of ovarian cancer stem cell-like cells leading to an increased tumor burden. Mol Cancer. 2013; 12:24. [PubMed: 23537295]
44. Colby AH, Colson YL, Grinstaff MW. Microscopy and tunable resistive pulse sensing characterization of the swelling of pH-responsive, polymeric expansile nanoparticles. Nanoscale. 2013; 5:3496–504. [PubMed: 23487041]
45. Colby AH, Liu R, Schulz MD, Padera RF, Colson YL, Grinstaff MW. Two-Step Delivery: Exploiting the Partition Coefficient Concept to Increase Intratumoral Paclitaxel Concentrations In vivo Using Responsive Nanoparticles. Sci Rep. 2016; 6:18720. [PubMed: 26740245]
46. Griset AP, Walpole J, Liu R, Gaffey A, Colson YL, Grinstaff MW. Expansile nanoparticles: synthesis, characterization, and in vivo efficacy of an acid-responsive polymeric drug delivery system. Journal of the American Chemical Society. 2009; 131:2469–71. [PubMed: 19182897]
47. Zubris KA, Colson YL, Grinstaff MW. Hydrogels as intracellular depots for drug delivery. Molecular pharmaceutics. 2012; 9:196–200. [PubMed: 22053709]
48. Zubris KA, Liu R, Colby A, Schulz MD, Colson YL, Grinstaff MW. In vitro activity of Paclitaxel-loaded polymeric expansile nanoparticles in breast cancer cells. Biomacromolecules. 2013; 14:2074–82. [PubMed: 23617223]
49. Griset AP, Walpole J, Liu R, Gaffey A, Colson YL, Grinstaff MW. Expansile Nanoparticles: Synthesis, Characterization, and *In vivo* Efficacy of an Acid-Responsive Polymeric Drug Delivery System. J Am Chem Soc. 2009; 131:2469–71. [PubMed: 19182897]
50. Herrera VL, Colby AH, Tan GA, Moran AM, O'Brien MJ, Colson YL, et al. Evaluation of expansile nanoparticle tumor localization and efficacy in a cancer stem cell-derived model of pancreatic peritoneal carcinomatosis. Nanomedicine (Lond). 2016; 11:1001–15. [PubMed: 27078118]
51. Yoo JW, Chambers E, Mitragotri S. Factors that control the circulation time of nanoparticles in blood: challenges, solutions and future prospects. Curr Pharm Des. 2010; 16:2298–307. [PubMed: 20618151]
52. Riehemann K, Schneider SW, Luger TA, Godin B, Ferrari M, Fuchs H. Nanomedicine--challenge and perspectives. Angew Chem Int Ed Engl. 2009; 48:872–97. [PubMed: 19142939]
53. Tanida I, Ueno T, Kominami E. LC3 and Autophagy. Methods Mol Biol. 2008; 445:77–88. [PubMed: 18425443]

54. Mohamed F, Marchettini P, Stuart OA, Sugarbaker PH. Pharmacokinetics and tissue distribution of intraperitoneal paclitaxel with different carrier solutions. Cancer chemotherapy and pharmacology. 2003; 52:405–10. [PubMed: 12879282]

55. Tsai M, Lu Z, Wang J, Yeh TK, Wientjes MG, Au JL. Effects of carrier on disposition and antitumor activity of intraperitoneal Paclitaxel. Pharmaceutical research. 2007; 24:1691–701. [PubMed: 17447121]

56. Au JL, Li D, Gan Y, Gao X, Johnson AL, Johnston J, et al. Pharmacodynamics of immediate and delayed effects of paclitaxel: role of slow apoptosis and intracellular drug retention. Cancer research. 1998; 58:2141–8. [PubMed: 9605758]

57. Mosesson Y, Mills GB, Yarden Y. Derailed endocytosis: an emerging feature of cancer. Nat Rev Cancer. 2008; 8:835–50. [PubMed: 18948996]

58. Lei H, Hofferberth SC, Liu R, Colby A, Tevis KM, Catalano P, et al. Paclitaxel-loaded expansile nanoparticles enhance chemotherapeutic drug delivery in mesothelioma 3-dimensional multicellular spheroids. J Thorac Cardiovasc Surg. 2015; 149:1417–25. [PubMed: 25841659]

59. Lu Z, Tsai M, Lu D, Wang J, Wientjes MG, Au JL. Tumor-penetrating microparticles for intraperitoneal therapy of ovarian cancer. J Pharmacol Exp Ther. 2008; 327:673–82. [PubMed: 18780831]

60. Mizushima N, Yoshimori T, Levine B. Methods in mammalian autophagy research. Cell. 2010; 140:313–26. [PubMed: 20144757]

61. Barth S, Glick D, Macleod KF. Autophagy: assays and artifacts. The Journal of pathology. 2010; 221:117–24. [PubMed: 20225337]

62. Gonzalez-Angulo AM, Hortobagyi GN. Optimal schedule of paclitaxel: weekly is better. J Clin Oncol. 2008; 26:1585–7. [PubMed: 18375889]

63. Mitchison TJ. The proliferation rate paradox in antimitotic chemotherapy. Mol Biol Cell. 2012; 23:1–6. [PubMed: 22210845]

64. Tan G, Heqing L, Jiangbo C, Ming J, Yanhong M, Xianghe L, et al. Apoptosis induced by low-dose paclitaxel is associated with p53 upregulation in nasopharyngeal carcinoma cells. Int J Cancer. 2002; 97:168–72. [PubMed: 11774260]

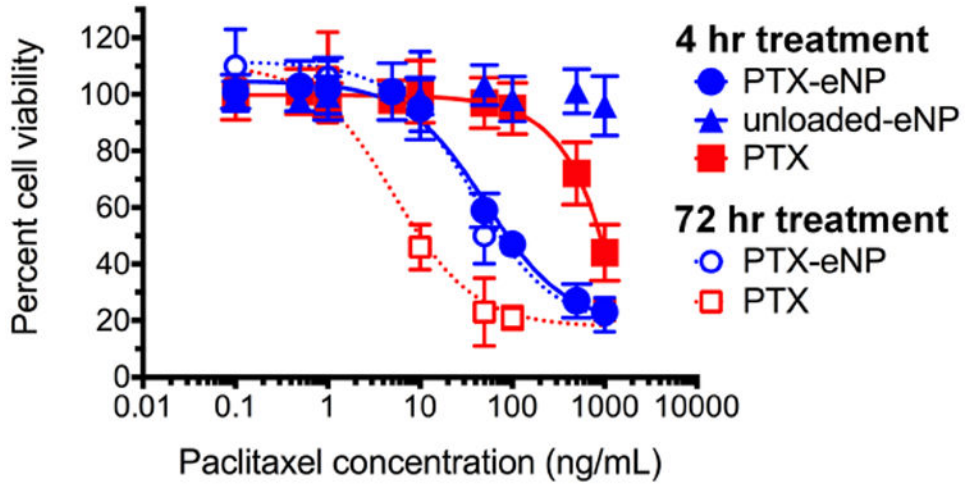

Fig. 1.

Cytotoxicity of PTX-eNPs against human malignant mesothelioma cells using both short (4 hr; solid lines) and long/continuous (72 hr; dashed lines) duration exposure to treatments. MSTO-211H tumor cells were treated with PTX-eNPs or equivalent concentrations of PTX for the designated exposure time before cell viability was assessed via MTS assay. PTX-eNPs were significantly more potent after a 4 hr exposure than PTX (IC_{50} = 44.6 ng/mL vs 1,009 ng/mL, respectively). Unloaded-eNPs are not cytotoxic at any concentrations tested. Data are shown as mean ± SD (n ≥ 3).

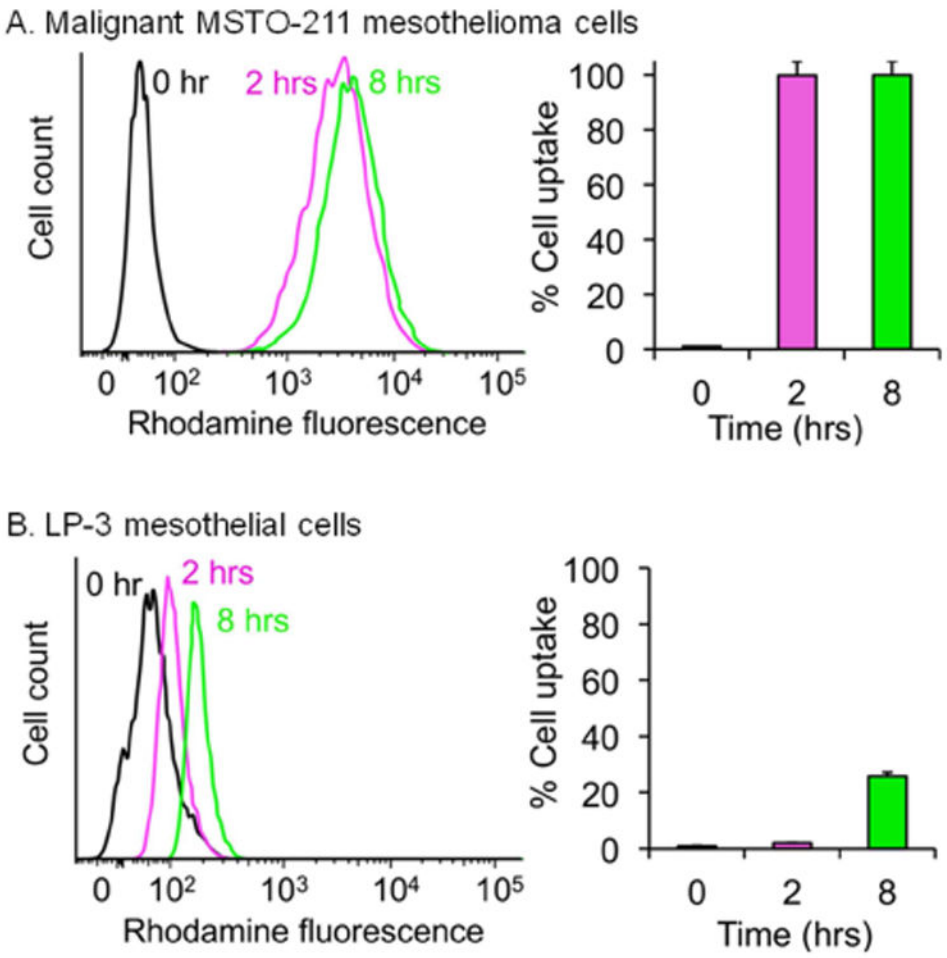

Fig. 2.

Kinetics of cellular uptake of eNPs in malignant and non-malignant mesothelial cell lines. Cells were treated with Rho-eNPs for 0 (control), 2 or 8 hrs before washing and flow cytometric analysis. (A) Rho-eNP signal in human-derived MSTO-211H mesothelioma tumor cells increases rapidly (>98% cells compared to control) within 2 hrs of incubation (pink). (B) Rho-eNP uptake is slower (2% at 2 hrs (pink), 28% at 8 hrs (green)) in non-malignant human mesothelial LP-3 cells. Data are shown as mean ± SD ($n \geq 3$).

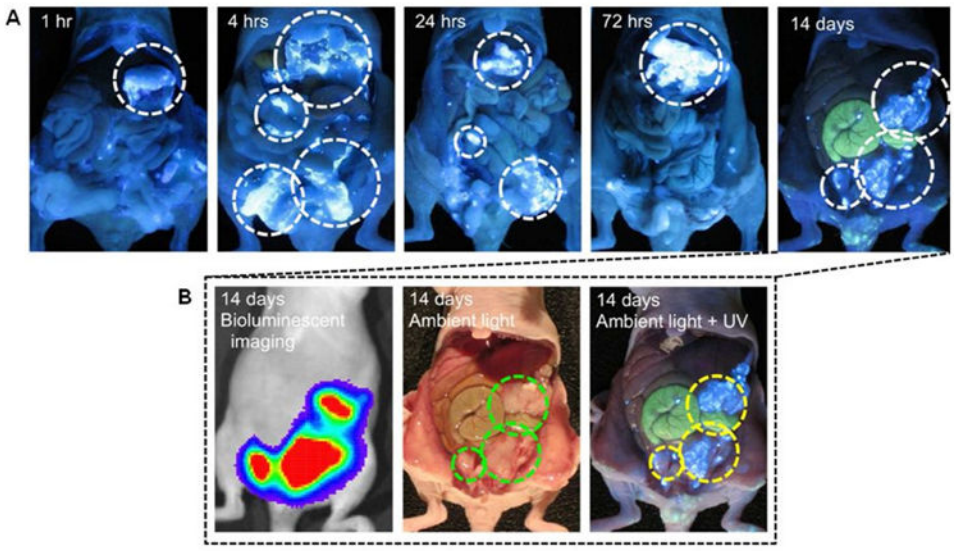

Fig. 3.

Kinetics of PF-eNP localization to intraperitoneal mesothelioma tumors in vivo. The PF-eNPs emit bright white-blue light under UV-excitation. (A) Co-localization of PF-eNPs and tumors (white circles) in individual animals begins within 1-4 hrs after intraperitoneal PF-eNP injection and becomes more intense over several days. (B) Live bioluminescent (left), post-mortem ambient light (middle), and ambient/UV light combination (right) demonstrate co-localization of tumor burden (green circles) and PF-eNPs (yellow circles). Images are representative of three animals at each time point.

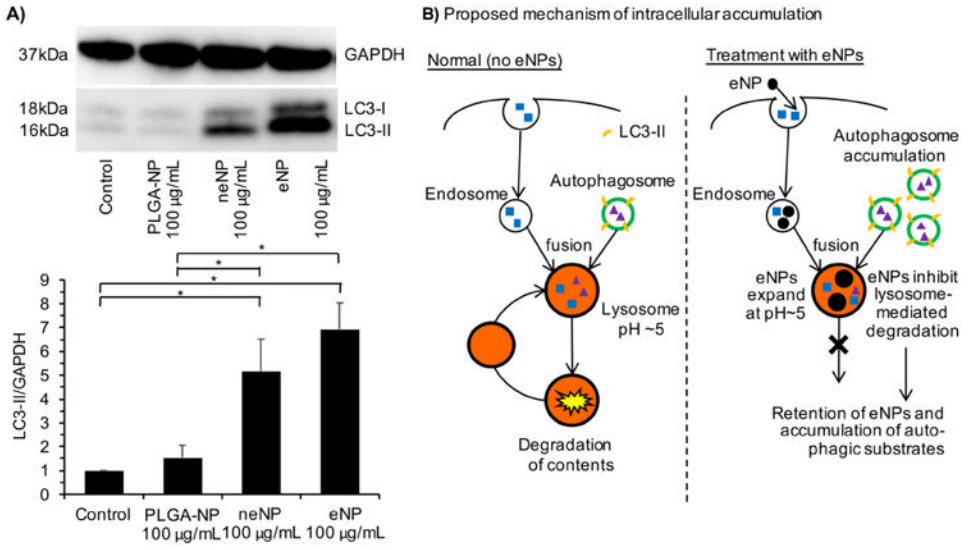

Fig. 4.

Quantification of LC3-II protein levels in eNP-treated cells by Western Blot. (A) Treatment of MSTO-211H tumor cells with PLGA-NPs does not significantly increase LC3-II levels compared to control. Treatment with eNPs and neNPs at 100 μg/mL significantly increases LC3-II levels, indicating the increased accumulation of autophagosomes. Results are normalized to the GAPDH protein level for each lane. Data are shown as mean ± SD (N = 5; * = $P < 0.05$). (B) Proposed mechanism by which eNPs (black filled circles) disrupt intracellular trafficking and lead to autophagosomal accumulation.

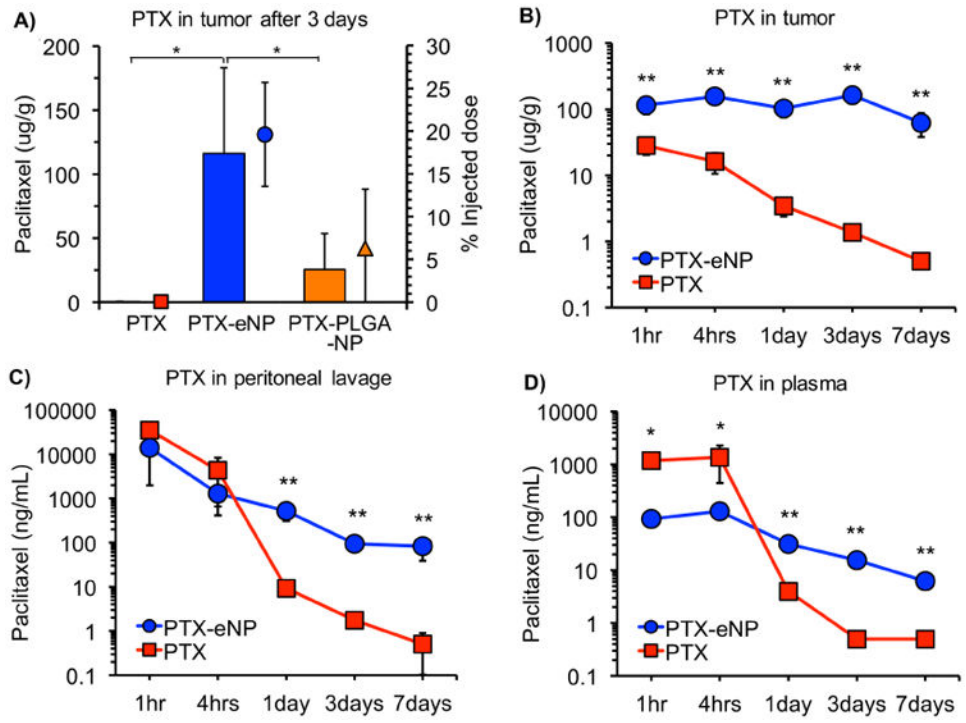

Fig. 5.

Paclitaxel concentrations in established tumor tissues, peritoneal lavage, and plasma after single bolus treatment injection given 14 days after inoculation with MSTO-211H tumor cells in NU/J mice. PTX-eNPs, PTX-PLGA-NPs or PTX (all at 10 mg/kg PTX dose) were injected intraperitoneally and tissues subsequently harvested for assessment of PTX levels. (A) PTX concentration in tumor tissues at 3 days ($n \geq 9$). Columns represent tissue concentrations. Dots and bars represent percentage of injected dose in tumor tissues. (B, C, D) PTX concentrations in tumor, peritoneal lavage, and plasma as a function of time ($n \geq 3$ per time point). Data are shown as mean ± SD (* $P < 0.05$, ** $P < 0.001$) Note: Tumor concentration data for PTX-eNPs in panel A was previously reported in [45] and is used for comparison. No other data from panels A, B, C, or D has been published.

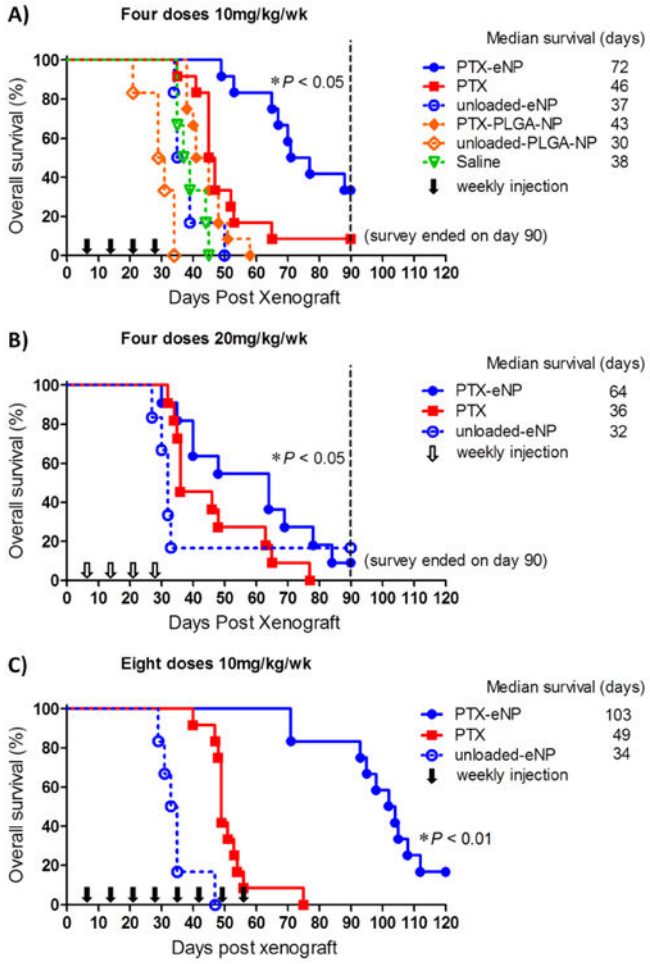

Fig. 6.

Impact of multi-dose PTX-eNP regimen on animal survival in a murine model of established intraperitoneal mesothelioma. (A) Four weekly IP doses of PTX-eNPs nearly doubles overall survival. Weekly intraperitoneal treatments (arrows) were initiated 7 days after 5 million MSTO-211H/luc cells were injected. Animals received 10 mg/kg/dose PTX in PTX-eNPs, PTX-PLGA-NPs, or PTX, or a matched control treatment of unloaded-eNPs, unloaded-PLGA-NPs, or saline (*$P < 0.05$). (B) Impact of doubling PTX dose on overall survival. Animals received 4 doses of 20 mg/kg PTX as PTX-eNPs or PTX, or unloaded-eNPs (* $P < 0.05$). (C) Impact of doubling the number of doses of PTX on overall survival. Animals received eight-doses of 10 mg/kg PTX in PTX-eNPs or PTX, or an unloaded-eNP control (* $P < 0.01$).